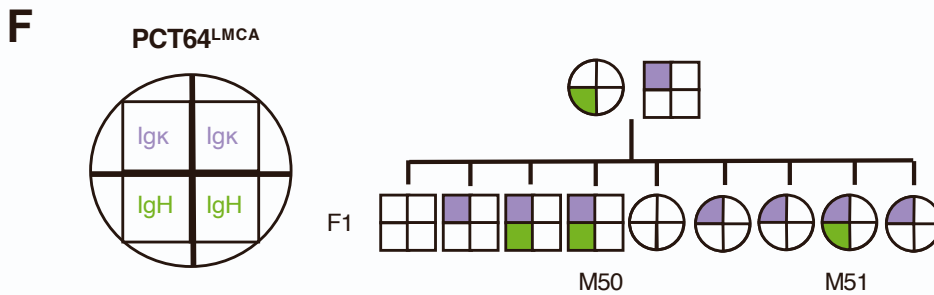
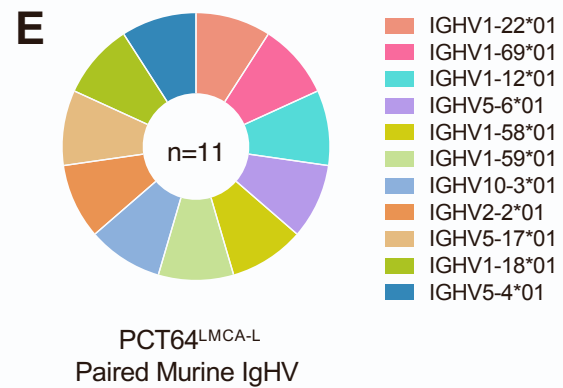
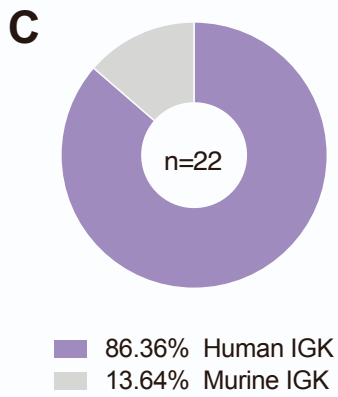
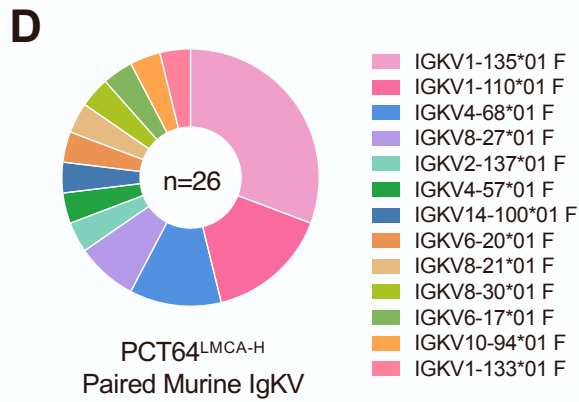
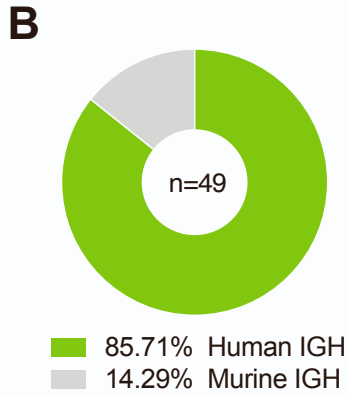
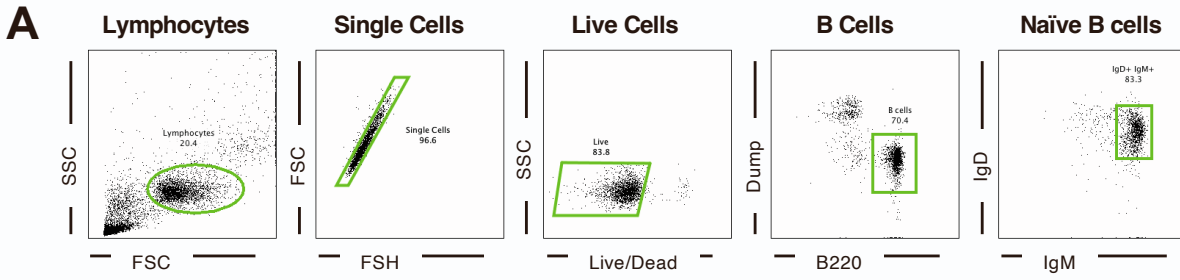


Supplemental information

**Membrane-bound mRNA immunogens lower the
threshold to activate HIV Env V2 apex-directed broadly
neutralizing B cell precursors in humanized mice**

Eleonora Melzi, Jordan R. Willis, Krystal M. Ma, Ying-Cing Lin, Sven Kratochvil, Zachary T. Berndsen, Elise A. Landais, Oleksandr Kalyuzhniy, Usha Nair, John Warner, Jon M. Steichen, Anton Kalyuzhniy, Amber Le, Simone Pecetta, Manfredo Perez, Kathrin Kirsch, Stephanie R. Weldon, Samantha Falcone, Sunny Himansu, Andrea Carfi, Devin Sok, Andrew B. Ward, William R. Schief, and Facundo D. Batista



G

Line	# litters	# pups	# knock-in (KI) pups			KI pup frequency (%)		
			H	κ	H, κ	H	κ	H, κ
LMCA	6	49	22	22	11	44.8	44.8	22.4

Figure S1. Generation of a human Ig least mutated common ancestor (LMCA) PCT64 knock-in mouse, related to Figure 1.

A. Flow cytometry gating strategy for sorting and sequencing single naïve B cell from knock-in mice generated with CRISPR-Cas9.

B. Pie chart showing frequency of amplified human PCT64 LMCA heavy chain (green) and murine heavy chain (grey), from single cell BCR sequencing of naïve B cells in PCT64^{LMCA} IGH mice (PCT64^{LMCA-H}) (n=49).

C. Pie chart shows frequency of amplified human PCT64 LMCA light chain (purple) and murine heavy chain (grey), from single cell BCR sequencing of naïve B cells in PCT64 LMCA IGK mice (PCT64^{LMCA-L}) (n=22).

D. PCT64^{LMCA-H} paired murine light chains V genes (n=26).

E. PCT64^{LMCA-L} paired murine heavy chains V genes (n=11).

F. Breeding schematic for PCT64^{LMCA-H} and PCT64^{LMCA-L} mouse line. Squares represent males and circles represent females. Upper halves indicate IGK and lower halves IGH, as per key at left.

G. Transmission frequency of IGH (H) and IGK (K) to the progeny.

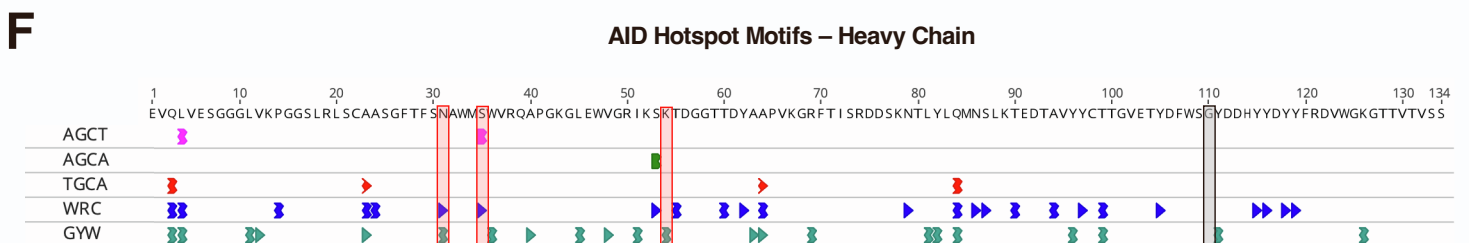
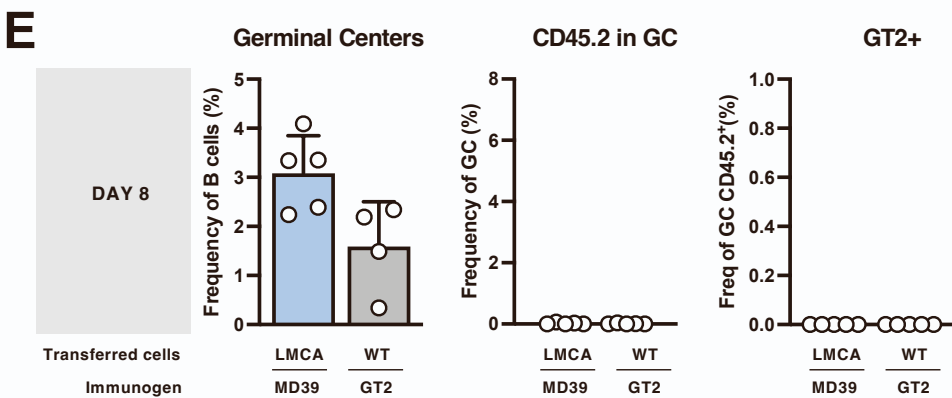
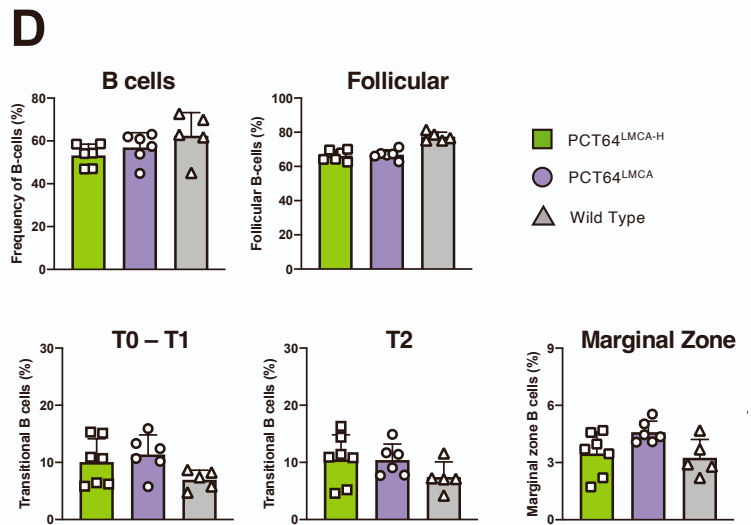
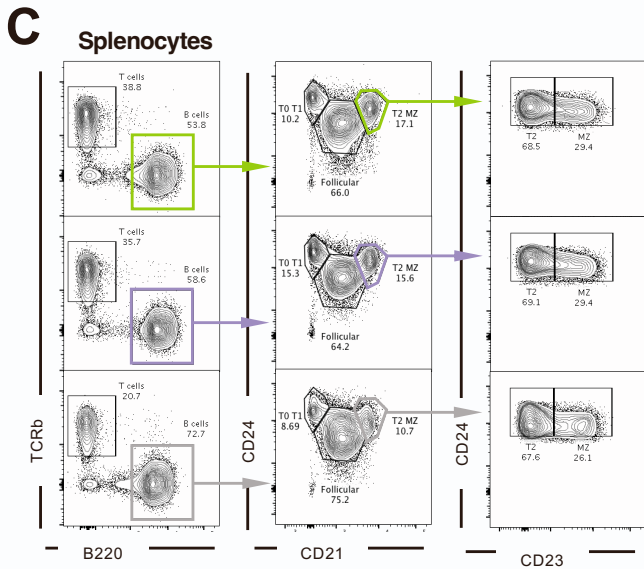
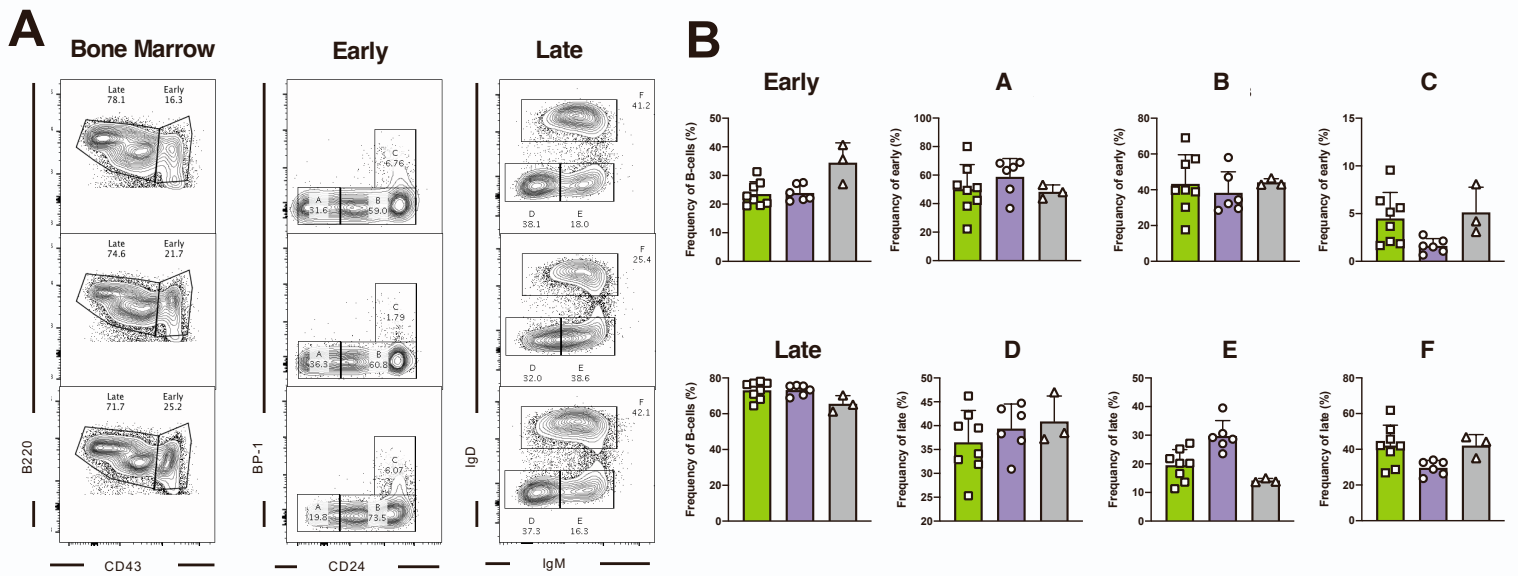


Figure S2. B lymphocyte development in PCT64^{LMCA-H} and PCT64^{LMCA} mice, related to Figures 1 and 2.

A. Representative FACS plots of bone marrow progenitor cells isolated from PCT64^{LMCA-H}, PCT64^{LMCA} and WT mice and gating strategy applied for the quantification of early (A, B and C) and late (D, E and F) subfraction of B cell developmental stages accordingly to (Hardy et al. 1991)

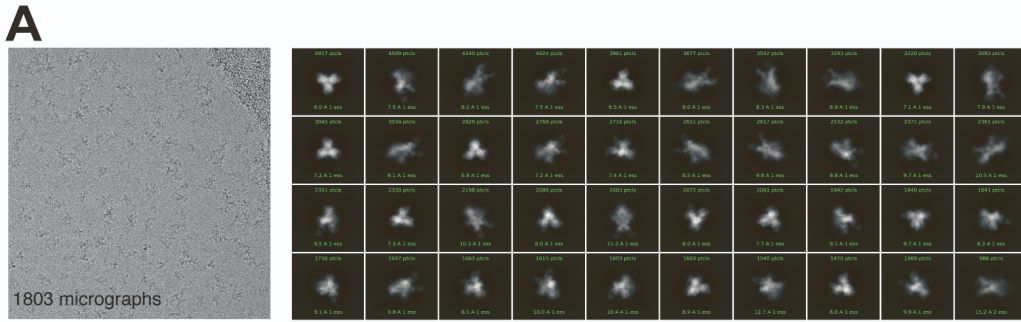
B. Quantification of early (A, B and C) and late (D, E and F) subfraction of B cell developmental stages in bone marrow from PCT64^{LMCA-H} (green), PCT64^{LMCA} (purple) and wild type (WT) (grey) mice (as in A). LMCA-H n=8, LMCA n=6, WT controls n=3. Data are presented as mean \pm SD.

C. Representative FACS plots of splenocytes isolated from PCT64^{LMCA-H}, PCT64^{LMCA} and WT mice and gating strategy applied for the quantification of splenic B cells and their differentiation into Follicular, Transitional (T0, T1, T2) and Marginal Zone B cells.

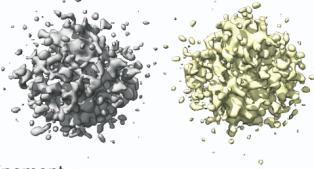
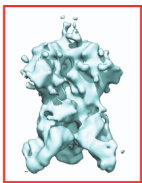
D. Quantification of splenic B cells and their differentiation into Follicular, Transitional (T0, T1, T2) and Marginal Zone B cells in spleens from PCT64^{LMCA-H} (green), PCT64^{LMCA} (purple) and Wild Type (grey) mice (as in C). LMCA and LMCA-H n=6, WT controls n=5. Data are presented as mean \pm SD.

E. Quantification of B cell responses in spleen at 8 days after immunization. CD45.1 WT mice received either 500,000 PCT64^{LMCA} B cells and were immunized with MD39-SOSIP trimers or received 500,000 wildtype CD45.2 B cells and were immunized with GT2 trimers. Experiments were performed in duplicate, one is shown (n=5). Data are presented as mean \pm SD.

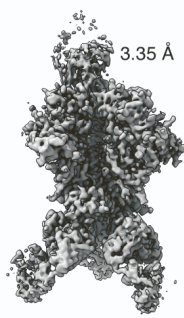
F. Analysis of the activation-induced deaminase (AID) enzyme binding sites in PCT64 LMCA heavy chain. AA position of enriched on-track mutations are highlighted (31, 35, 52b, 100d).



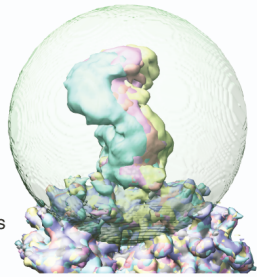
B ↓ ab-initio classification (171960)



↓ NU-refinement + CTF refinement (108627)



→ 3D variability + clustering into 6 classes



↓ 3 clusters with similar Fab orientation selected
NU-refinement + CTF refinement (62971)

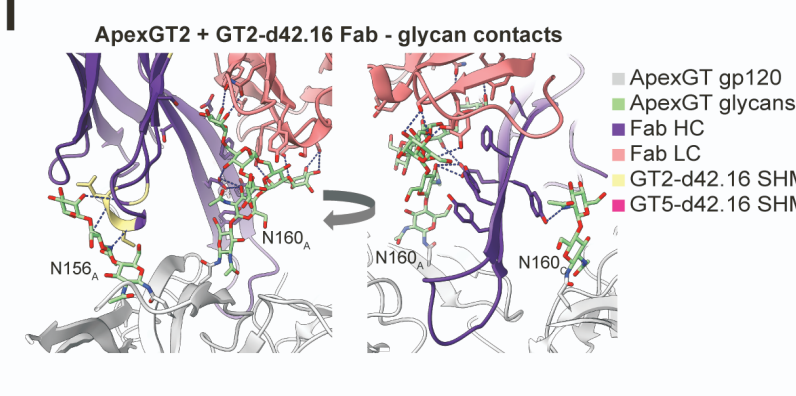
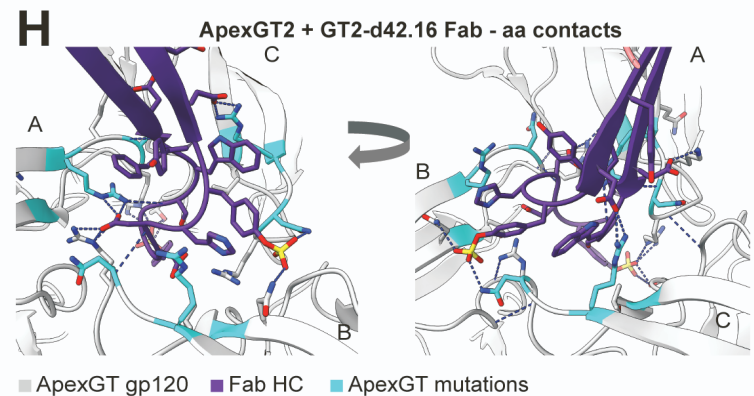
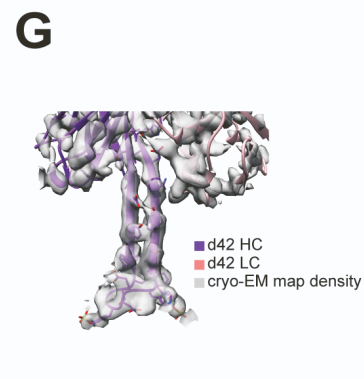
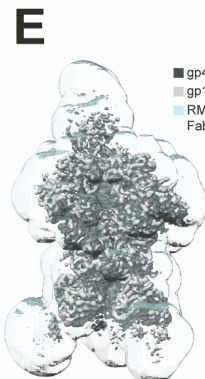
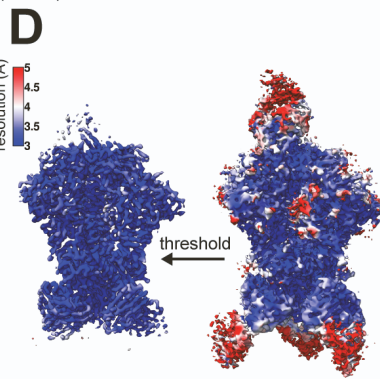
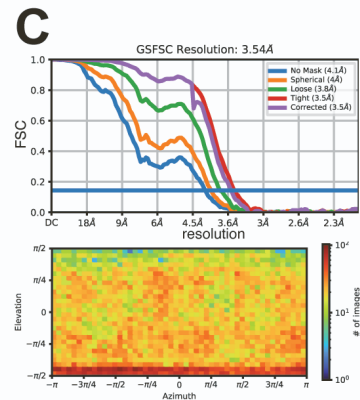
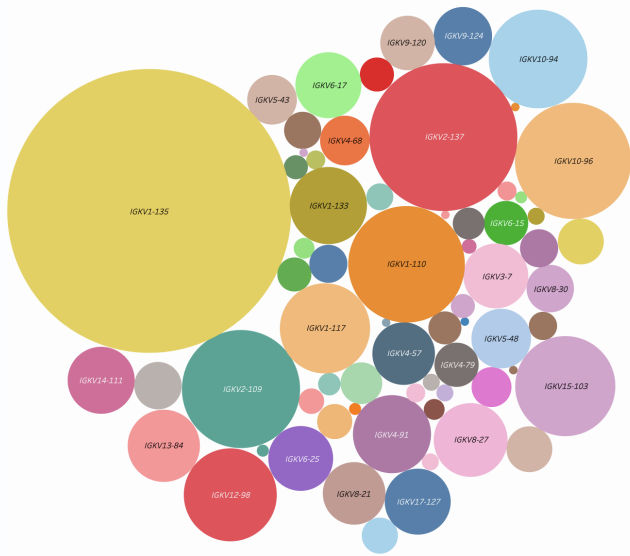


Figure S3. Cryo-EM data processing workflow for ApexGT2 in complex with GT2-d42.16

Fab, related to Figure 2.

- A. Raw EM micrograph and 2-D class averages of selected particles.
- B. 3-D data processing workflow.
- C. Fourier shell correlation and angular distribution plots.
- D. Local resolution estimates.
- E. Mask used for refinement and sharpening.
- F. Map segmentation.
- G. Isolated cryo-EM map density within a 3Å radius around Fab residues.
- H. Close up of the epitope/paratope region of ApexGT2 + G2-d42.16 showing hydrogen-bonding interactions with gp120 amino acid residues.
- I. Close up of the epitope/paratope region of ApexGT2 + GT2-d42.16 showing hydrogen-bonding interactions with ApexGT2 glycans.

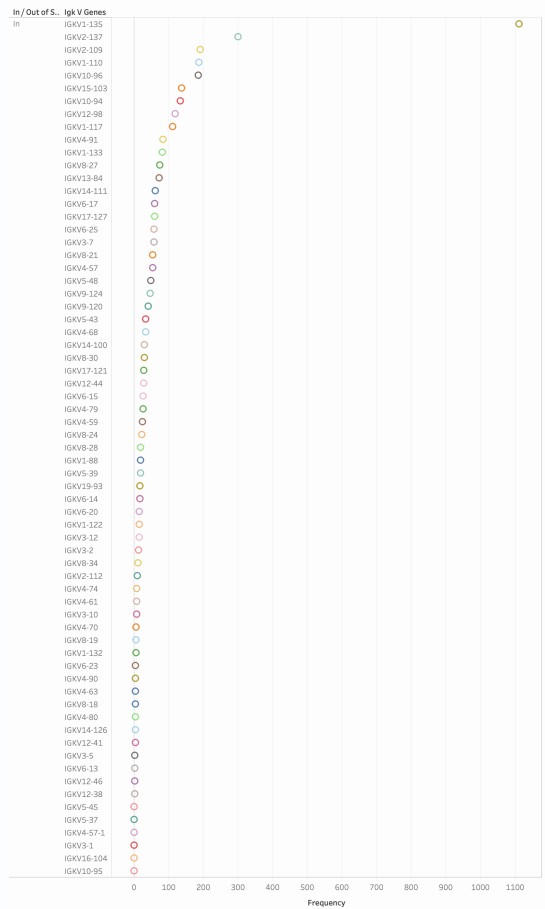
A Frequency and diversity of IHK V genes paired with PCT64uca IGH



B Frequency and diversity of IgK V genes paired with murine IgH

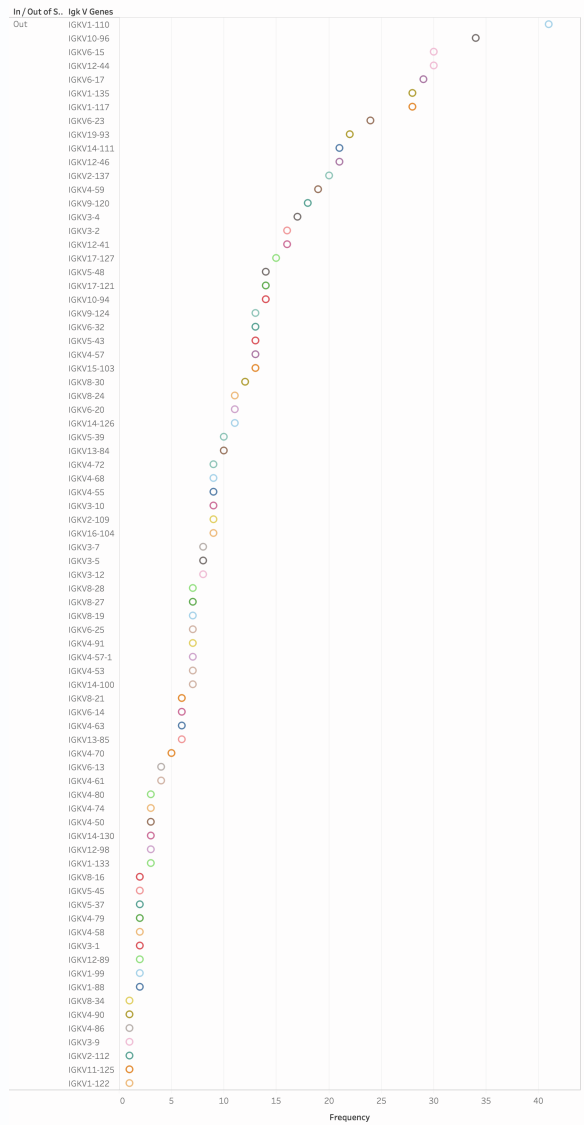


PCT64 IgK



- IGKV1-88
- IGKV1-110
- IGKV1-117
- IGKV1-122
- IGKV1-132
- IGKV1-133
- IGKV1-135
- IGKV2-109
- IGKV2-112
- IGKV2-117
- IGKV2-137
- IGKV3-1
- IGKV3-2
- IGKV3-5
- IGKV3-7
- IGKV3-10
- IGKV3-12
- IGKV4-1
- IGKV4-2
- IGKV4-5
- IGKV4-7
- IGKV4-10
- IGKV4-12
- IGKV4-15
- IGKV4-17
- IGKV4-20
- IGKV4-23
- IGKV4-25
- IGKV4-28
- IGKV4-31
- IGKV4-34
- IGKV4-37
- IGKV4-41
- IGKV4-43
- IGKV4-45
- IGKV4-48
- IGKV4-51
- IGKV4-54
- IGKV4-57
- IGKV4-61
- IGKV4-63
- IGKV4-68
- IGKV4-71
- IGKV4-74
- IGKV4-79
- IGKV4-80
- IGKV4-90
- IGKV4-91
- IGKV5-37
- IGKV5-39
- IGKV5-43
- IGKV5-45
- IGKV5-48
- IGKV5-13
- IGKV5-14
- IGKV5-15
- IGKV5-17
- IGKV5-20
- IGKV5-23
- IGKV5-25
- IGKV5-28
- IGKV5-19
- IGKV5-21
- IGKV5-24
- IGKV5-27
- IGKV5-28
- IGKV5-30
- IGKV5-34
- IGKV5-124
- IGKV5-124
- IGKV5-94
- IGKV5-95
- IGKV5-96
- IGKV5-123
- IGKV5-124
- IGKV5-126
- IGKV5-127
- IGKV5-128
- IGKV5-129
- IGKV5-130
- IGKV5-131
- IGKV5-132
- IGKV5-133
- IGKV5-134
- IGKV5-135
- IGKV5-136
- IGKV5-137
- IGKV5-138
- IGKV5-139
- IGKV5-140
- IGKV5-141
- IGKV5-142
- IGKV5-143
- IGKV5-144
- IGKV5-145
- IGKV5-146
- IGKV5-147
- IGKV5-148
- IGKV5-149
- IGKV5-150
- IGKV5-151
- IGKV5-152
- IGKV5-153
- IGKV5-154
- IGKV5-155
- IGKV5-156
- IGKV5-157
- IGKV5-158
- IGKV5-159
- IGKV5-160
- IGKV5-161
- IGKV5-162
- IGKV5-163
- IGKV5-164
- IGKV5-165
- IGKV5-166
- IGKV5-167
- IGKV5-168
- IGKV5-169
- IGKV5-170
- IGKV5-171
- IGKV5-172
- IGKV5-173
- IGKV5-174
- IGKV5-175
- IGKV5-176
- IGKV5-177
- IGKV5-178
- IGKV5-179
- IGKV5-180
- IGKV5-181
- IGKV5-182
- IGKV5-183
- IGKV5-184
- IGKV5-185
- IGKV5-186
- IGKV5-187
- IGKV5-188
- IGKV5-189
- IGKV5-190
- IGKV5-191
- IGKV5-192
- IGKV5-193

Mouse V (2)



- IGKV1-88
- IGKV1-99
- IGKV1-110
- IGKV1-117
- IGKV1-122
- IGKV1-133
- IGKV1-135
- IGKV2-109
- IGKV2-112
- IGKV2-137
- IGKV3-1
- IGKV3-2
- IGKV3-4
- IGKV3-5
- IGKV3-7
- IGKV3-9
- IGKV3-10
- IGKV3-12
- IGKV3-15
- IGKV3-21
- IGKV3-41
- IGKV3-55
- IGKV3-57
- IGKV3-58
- IGKV3-59
- IGKV3-61
- IGKV3-63
- IGKV3-68
- IGKV3-70
- IGKV3-72
- IGKV3-74
- IGKV3-79
- IGKV3-90
- IGKV3-86
- IGKV3-90
- IGKV3-91
- IGKV3-37
- IGKV3-39
- IGKV3-43
- IGKV3-45
- IGKV3-48
- IGKV3-13
- IGKV3-14
- IGKV3-15
- IGKV3-17
- IGKV3-20
- IGKV3-23
- IGKV3-25
- IGKV3-32
- IGKV3-32
- IGKV3-16
- IGKV3-19
- IGKV3-21
- IGKV3-24
- IGKV3-27
- IGKV3-28
- IGKV3-30
- IGKV3-34
- IGKV3-120
- IGKV3-124
- IGKV3-94
- IGKV3-96
- IGKV3-125
- IGKV3-41
- IGKV3-44
- IGKV3-46
- IGKV3-89
- IGKV3-84
- IGKV3-85
- IGKV3-100
- IGKV3-111
- IGKV3-111
- IGKV3-111
- IGKV3-130
- IGKV3-130
- IGKV3-103
- IGKV3-104
- IGKV3-104
- IGKV3-121
- IGKV3-127
- IGKV3-93

Figure S4. Light chain repertoire characterization in PCT64^{LMCA-H} mice, related to

Figure 3.

A. Bubble graph representing frequency and diversity of murine IGK V genes paired with PCT64 IGH in a naïve PCT64^{LMCA-H} mouse (n=3888). Bubble size represent relative frequency, colors indicate different V gene. Below, detailed legend of all the isolated IGK V genes and relative frequency.

B. Bubble graph representing frequency and diversity of murine IGK V genes paired with murine IGH in a naïve PCT64^{LMCA-H} mouse (n=815). Bubble size represent relative frequency, colors indicate different V gene. Below, detailed legend of all the isolated IGK V genes and relative frequency.

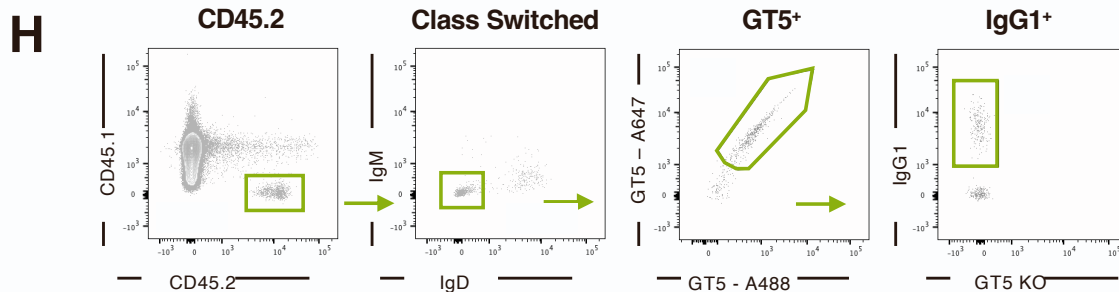
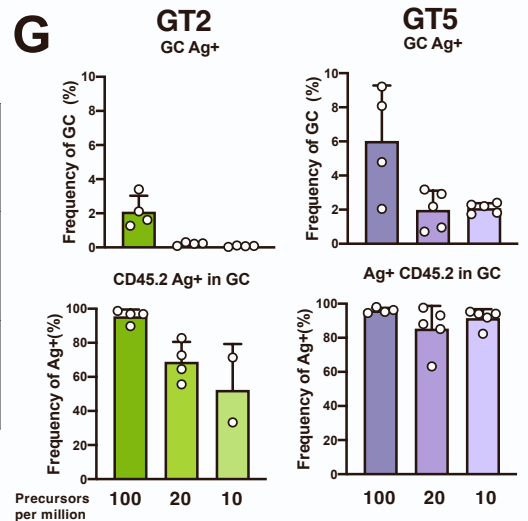
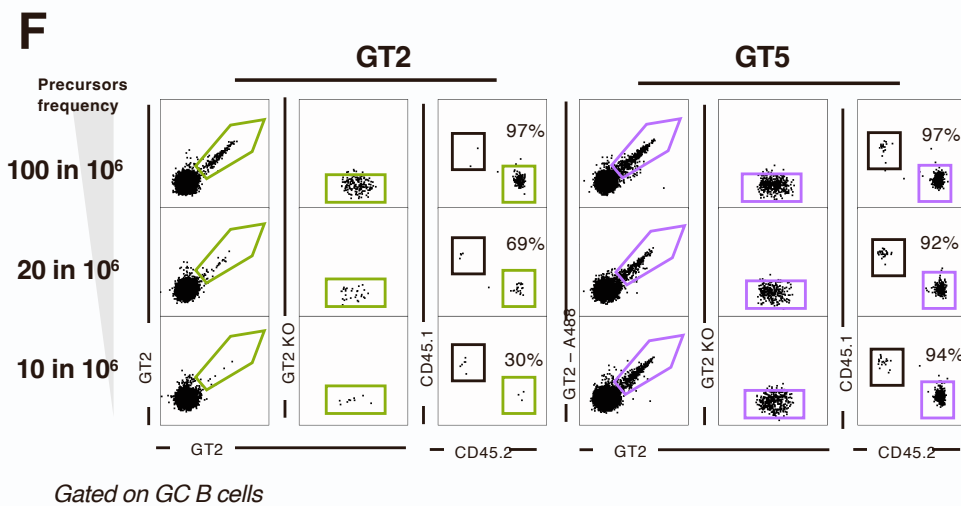
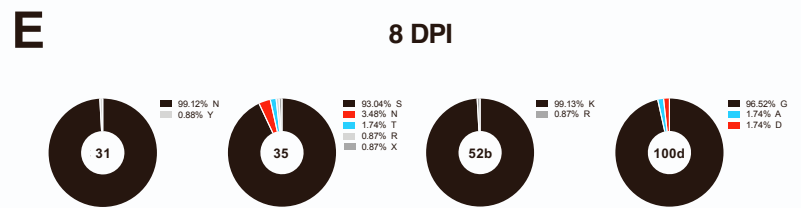
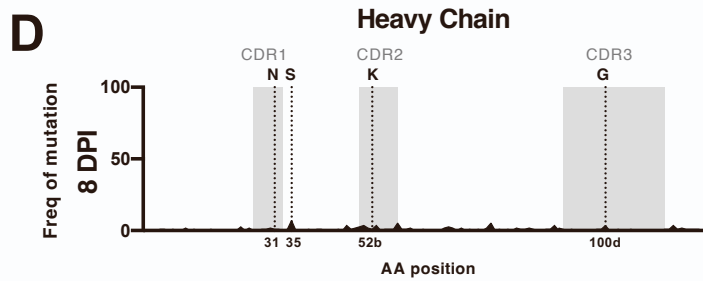
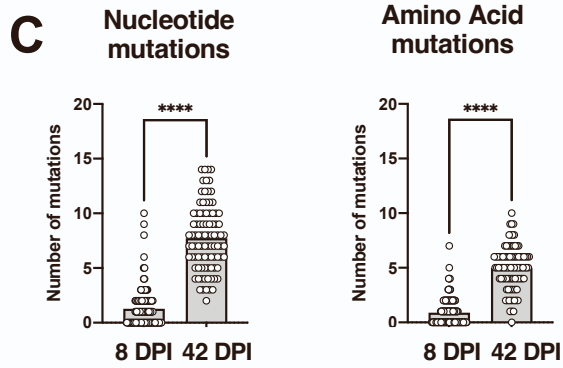
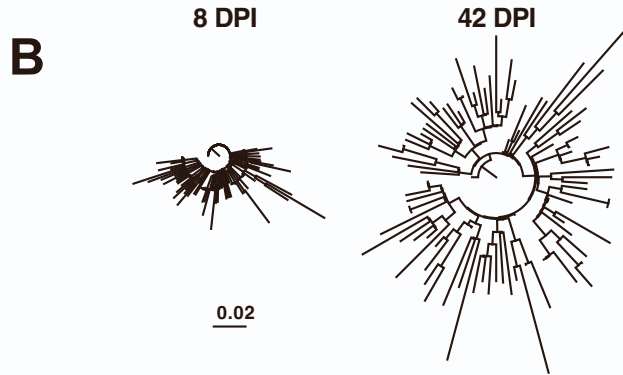
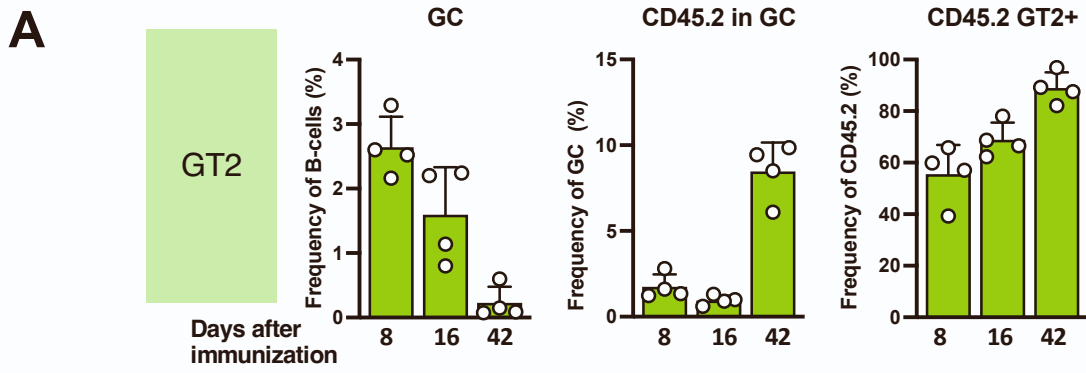


Figure S5. GT2 immunization activates PCT64 heavy chain with different light chains and GC competition after GT2 and GT5 immunization, related to Figures 3, 4 and 5.

A. FACS quantification of germinal center (GC) responses, CD45.2 cells inside GC, and GT2 binding B cells at 8, 16 and 42 days after immunization with GT2. Recipient mice received 500,000 CD45.2⁺ PCT64^{LMCA-H} B cells and responses were analyzed in the spleen. Experiments were performed in triplicate, one is shown (n=4/group). Data are presented as mean \pm SD.

B. Phylogenetic clonal lineage trees showing diversification of the PCT64^{LMCA} IGH from day 8 to day 42 after immunization. Branch length is representative of sequence distance.

C. Number of total nucleotide and amino acid mutations acquired in PCT64^{LMCA-H} heavy chain V genes (IGHV) at 8 (n=114) and 42 (n=106) DPI. P values calculated by Mann-Whitney test, ****P < 0.0001.

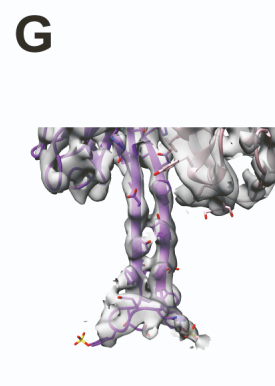
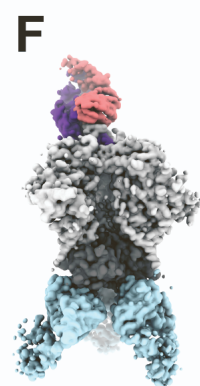
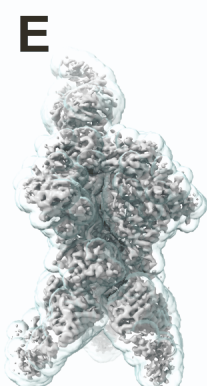
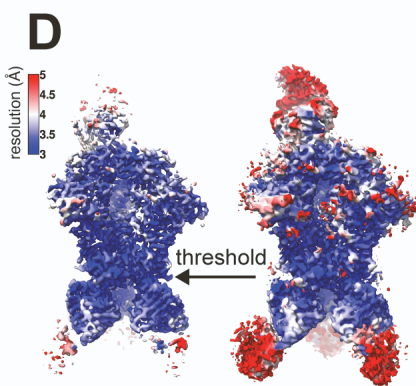
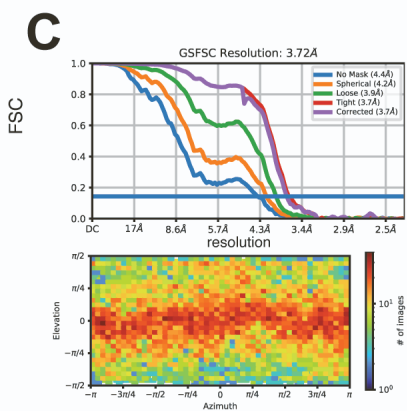
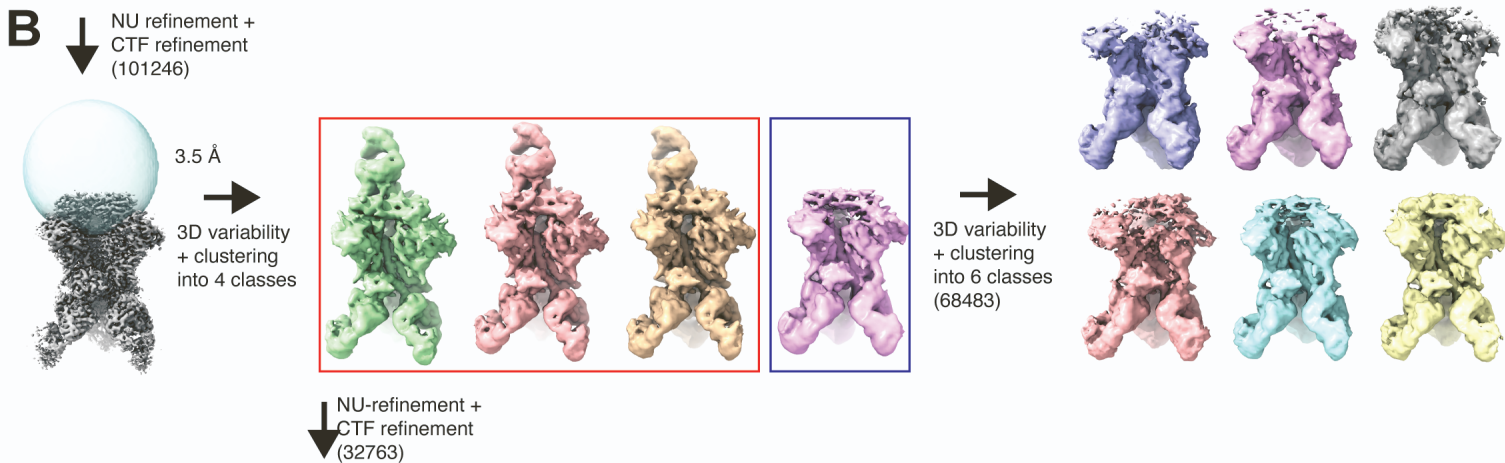
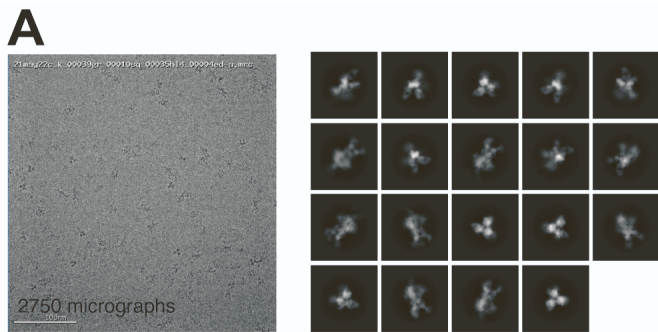
D. Frequencies of heavy chain AA mutations observed per residue at day 8 post-immunization in PCT64^{LMCA} heavy chain. HCDRs are highlighted in gray.

E. Distribution of selected PCT64 LMCA B cell heavy chain aa mutations in positions 31, 35, 52b and 100d at 8 dpi. Mutations present in mature PCT64 are in red, mutations present in PCT64-lineage early isolates are in blue, original LMCA amino acids are in black, other mutations are in grey.

F. Representative FACS plots of antigen-specific germinal center responses after immunization with GT2 (green) or GT5 (purple) (10 ug, adjuvanted with Sigma) in mice with 100, 20 and 10 per 10⁶ PCT64^{LMCA} precursor B cells.

G. Quantification of responses in F. Experiments were performed in triplicate, one is shown (n=4, for GT5 10,20:10⁶ n=5). Data are presented as mean \pm SD.

H. FACS gating strategy for sorting of class switched antigen specific cells at 42 dpi.



■ gp41 ■ d42 HC ■ RM20A3 ■ cryo-EM map density
 ■ gp120 ■ d42 LC ■ Fab ■ d42 HC ■ d42 LC

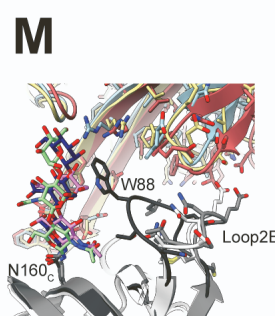
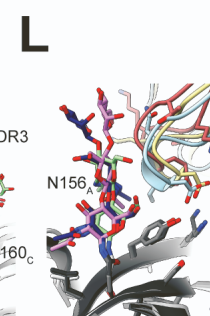
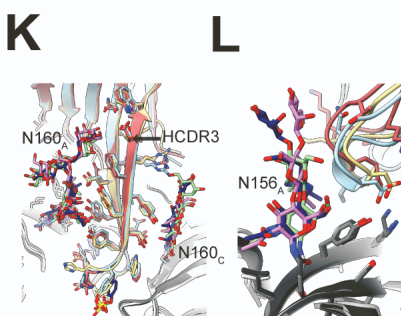
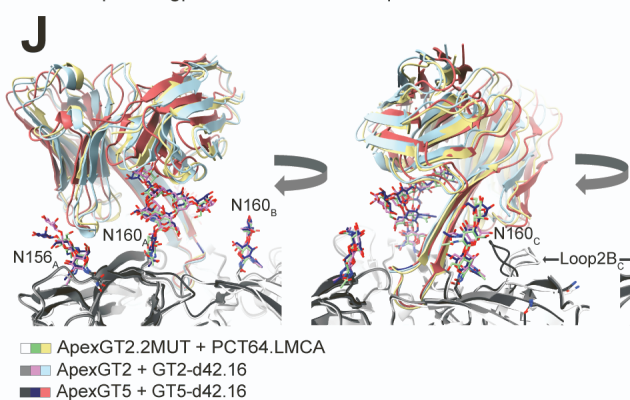
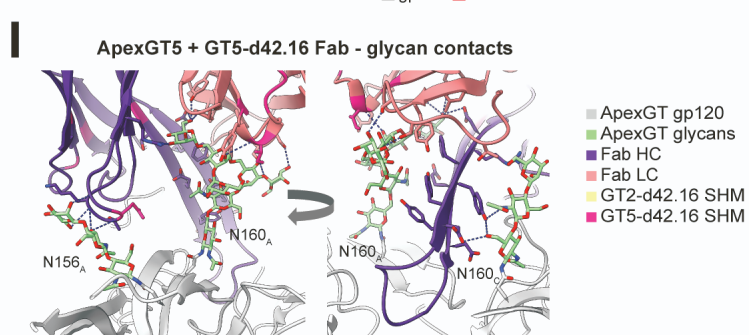
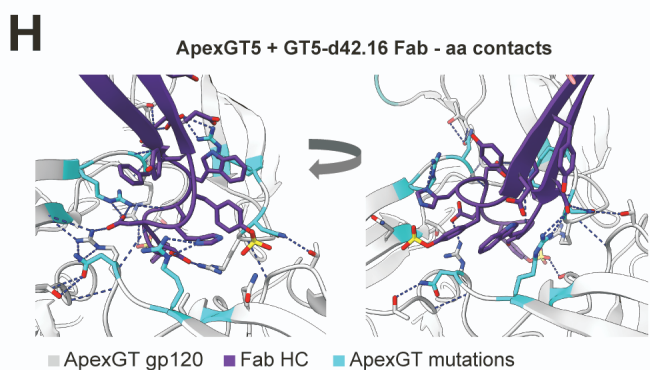


Figure S6. Cryo-EM data processing workflow for ApexGT5 in complex with GT5-d42.16 Fab, related to Figure 5.

- A. Raw EM micrograph and 2-D class averages of selected particles.
- B. 3-D data processing workflow.
- C. Global Fourier shell correlation and angular distribution plots.
- D. Local resolution estimates.
- E. Mask used for refinement and sharpening.
- F. Map segmentation.
- G. Isolated cryo-EM map density within a 3Å radius around Fab residues.
- H. Close up of the epitope/paratope region of ApexGT5 + GT5-d42.16 showing hydrogen bonding interactions with gp120 amino acid residues.
- I. Close up of the epitope/paratope region of ApexGT5 + GT5-d42.16 showing hydrogen bonding interactions with ApexGT2 glycans
- J. Structures of ApexGT2.2MUT + PCT64.LMCA, ApexGT2 + GT2-d42.16, and ApexGT5 + GT5-d42.16 aligned and overlaid viewed from 3 different angles.
- K. Close up of the HCDR3 domains and N160gp120A and B glycans,
- L. N156gp120A glycan,
- M. And loop2B of protomer C along with N160gp120A glycan.

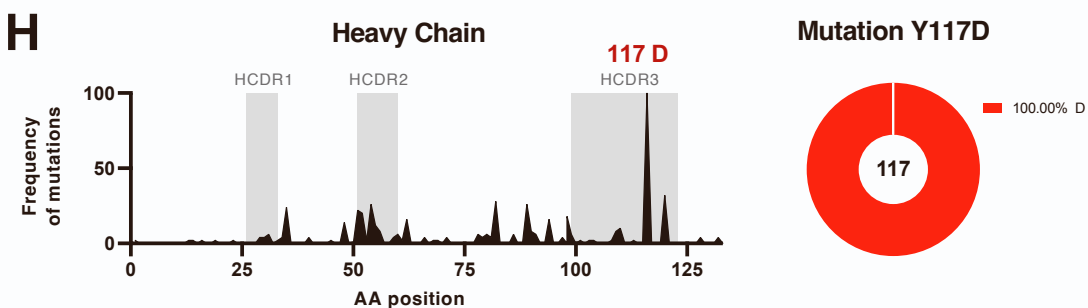
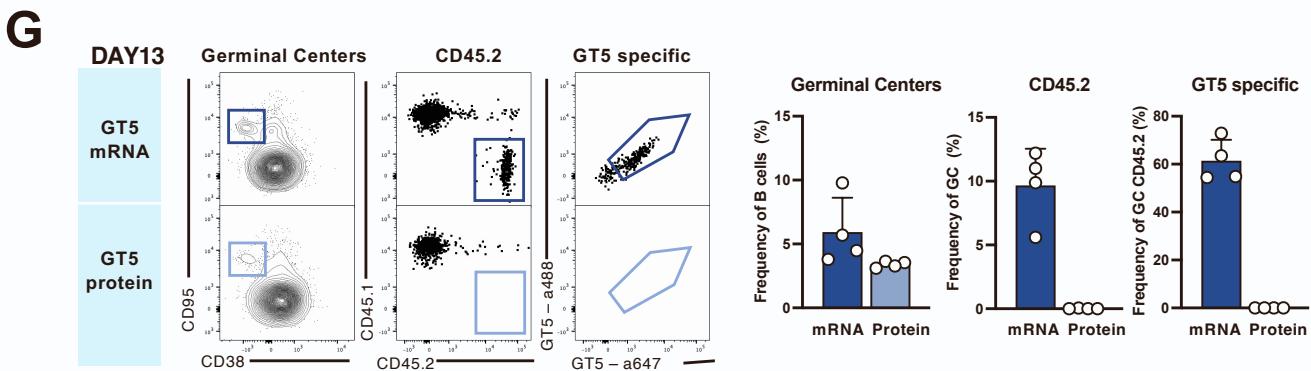
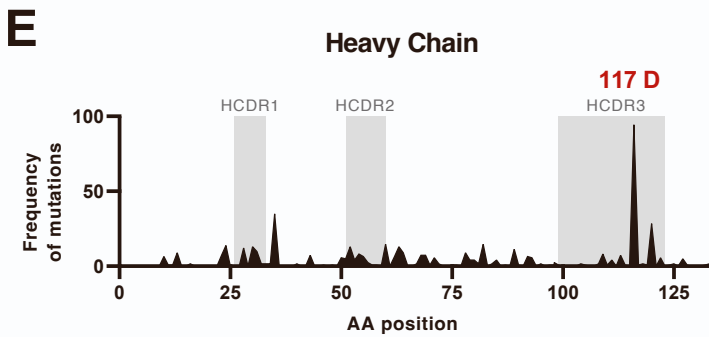
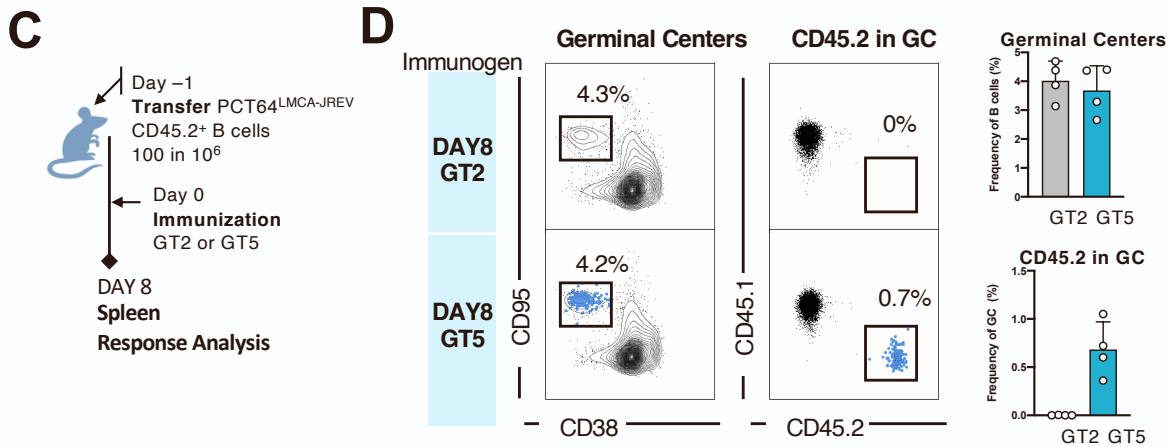
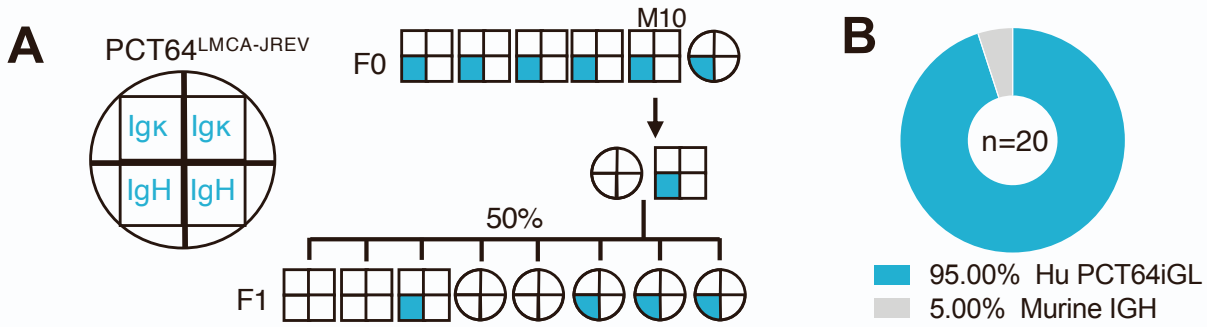


Figure S7. Generation of a PCT64 LMCA.JREV mouse and immunization strategies, related to Figure 7.

A. Breeding and transmission of the knock-in IGH PCT64^{LMCA.JREV} to the progeny.

B. Pie chart showing frequency of amplified human PCT64^{LMCA.JREV} heavy chain (teal) and murine heavy chain (grey), from single cell BCR sequencing of naïve B cells in a PCT64^{LMCA.JREV} IGH (PCT64^{LMCA.JREV-H}) (n=20) mouse (M10).

C. Schematic of immunization study design. Recipient mice received 100 PCT64^{LMCA.JREV} per10⁶ B cells and were immunized IP with either GT2 or GT5 trimers, responses were analyzed 8 dpi.

D. FACS plots of germinal centers (GC) responses at 8 dpi after immunization with GT2 or GT5 (left). Quantification of CD45.2 responses in GC (right) (n=4). Experiments were performed in duplicate, one is shown. Data are presented as mean ± SD.

E. Localization of sites of mutation enrichment in the IGH of CD45.2 B cell isolated 42 days after GT5 protein immunization.

F. HCDR3 alignment of PCT64 LMCA, LMCA.JREV and consensus of mutations acquired 42 days after GT5 immunization.

G. FACS analysis of GC responses 13 days after IM immunization with either GT5 mRNA or GT5 soluble protein in PCT64^{LMCA.JREV} recipient mice, quantification is on the right (n=4). Experiments were performed in triplicate, one is shown. Data are presented as mean ± SD.

H. Localization of sites of mutation enrichment in the IGH of CD45.2 B cell isolated 42 days after GT5 mRNA immunization (left). Pie chart with frequency of mutation Y117D (100% of 50 isolated IGH) (right).